Phosphate backbone neutralization increases duplex DNA flexibility: A model for protein binding

Tamara M. Okonogi*, Stephen C. Alley*†, Eric A. Harwood*†, Paul B. Hopkins*, and Bruce H. Robinson*‡

*Department of Chemistry, Box 351700, University of Washington, Seattle, WA 98195-1700; and †Pathogenesis, 201 Elliott Avenue West, Suite 150, Seattle, WA 98119

Communicated by Leonard S. Lerman, Massachusetts Institute of Technology, Cambridge, MA, February 5, 2002 (received for review May 27, 2001)

An important component of protein–DNA recognition is the charge neutralization of DNA backbone phosphates and subsequent protein-induced DNA bending. Replacement of phosphates by neutral methylphosphonates has previously been shown to be a model for protein-induced bending. In addition to bending, the neutralization process may change the inherent flexibility of the DNA—a feature never before tested. We have developed a method to measure the differential flexibility of duplex DNA when methylphosphonate substitutions are made and find that the local flexibility is increased up to 40%. These results imply that backbone-neutralization-dependent DNA flexibility augments DNA-binding motifs in protein–DNA recognition processes.

electrostatics | DNA bending | methylphosphonate | phantom proteins

Twenty years ago, Mirzabekov and Rich suggested that neutralization of the phosphate backbone of duplex DNA by cationic amino acids contributed to the bending and flexibility of DNA bound to histones (1). Recently this idea has been tested by using model systems in which specific phosphates on DNA have been neutralized (2–4) by replacing phosphate groups with methylphosphonates (MPs). It was shown that strategically placed runs or patches of MPs induced bends of 3–4° per base pair in DNA. The magnitude of bends induced in DNA upon binding positively charged mutants of GCN4, a bZIP transcription factor, compared favorably with the bends generated in the unbound DNA by substituting equal numbers of MPs for phosphates adjacent to the basic region in GCN4 (5). These and other examples (5–7) illustrate the significant contribution of charge-neutralization-induced DNA bending to the binding energetics of protein recognition processes.

Increased DNA flexibility could contribute to the energetics of protein–DNA binding by allowing the DNA to accommodate a greater degree of bending and a wider range of structural conformations at the same energy. Transient electric birefringence studies of meroduplexes (in which one side of the duplex DNA has no sugar-phosphate backbone and no charge) found no bends between base pairs (6° per base pair is the lower detection limit of the experiment) but found a suggestion of increased flexibility (8). Theoretical estimates indicate that the electrostatic contribution to the static bending ranges from negligible (9–11) to about a 5° bend per base pair (12). Theoretical estimates of the electrostatic contribution to the dynamic bending also range from increased flexibility (1, 2) through a negligible effect on flexibility (13, 14) to reduced flexibility (15), heightening the importance of experimentally testing whether MP-modified DNA actually alters the internal flexibility of duplex DNA. This report demonstrates that MP substitution does increase the flexibility and that the increased flexural root-mean-square (rms) bending is comparable to the mean bend induced by the MP substitution. The entropic and electrostatic contributions attributable to MP substitution are also investigated.

Site-specific duplex DNA flexibility and differential flexibility attributable to changes in structure have not been experimentally quantified before largely because of technical limitations. Continuous-wave electron paramagnetic resonance (CW-EPR) spectroscopy (16, 17), in combination with a site-specific base pair, composed of 2-aminopurine (**P**) and a spin-labeled nitroxide quinolone (**Q**) (18–20), is used to investigate the submicrosecond flexibility of duplex DNA with and without MP substitution. The probe is part of the sixth base pair (**P·Q**) in the duplex and monitors the dynamics of the DNA at this position. Flexibility of the *i*th base pair is characterized by an order parameter, S_i, which is related to the total mean squared internal oscillation amplitude, $\langle\beta_i^2\rangle$. S_i is measured by the EPR experiment in the following manner: In the absence of flexure, the width of the EPR spectrum of a nitroxide is characterized as A_{zz}, the major element of the nuclear spin interaction tensor, **A**. Rapid oscillation attributable to flexure of the DNA produces a smaller, averaged width $\langle A_{zz}\rangle$. The order parameter is related to the mean square oscillation and the observed EPR spectral widths by

$$S_i \approx 1 - \frac{3}{2}\langle\beta_i^2\rangle = \frac{\langle A_{zz}\rangle - \bar{a}}{A_{zz} - \bar{a}}, \qquad [1]$$

where $\bar{a}$ is a known constant, and is independent of probe motion (20).

The mean squared oscillation amplitude, $\langle\beta_i^2\rangle$, is connected to the flexural dynamics of the bases according to the weakly bending rod (WBR) theory (16, 17, 21, 22) for duplex DNA. The WBR theory assumes that bending of a base pair in duplex DNA relative to each of its neighbors obeys Hooke's law. The potential of interaction is characterized by a bending force constant, κ_i, which, in principle, could be unique for each base pair within a context of its neighbors, which may include many base pairs in the immediate vicinity. The form of the WBR model used here does not take into account the sequence-dependent nature of the bases, and therefore this model may not fully explain all of the data. In part, the neglect of sequence is consistent with the observations of Strauss and Maher, who found that ". . . [static] bending induced by MP substitution is independent of the precise sequence context. . . " (2, 4). We included the effects of static bends in the DNA introduced by the MP substitutions in the analysis of the flexibility. Although permanent bends do not appreciably alter communication of the internal bending modes among bases (16), a permanent bend in the DNA molecule changes the magnitude and orientation of the diffusion elements of the uniform modes with respect to the probe. This can affect the measured value of $\langle\beta_i^2\rangle$, altering the interpretation of the dynamics seen at the probe (16). However, the recalculated uniform modes (23) for all DNAs examined here, with and without the displacements induced by the MP substitutions, were found to be nearly identical.

Abbreviations: MP, methyl phosphonate; **P**, 2-aminopurine; **Q** (a spin-labeled nitroxide quinolone), 3-(2-deoxy-β-D-*erythro*-pentofuranosyl)-1,2,6,8-tetrahydro-6,6,8,8-tetramethyl-2-oxo-7*H*-pyrrolo[3,4-g]quinolin-7-xyloxy; UNB, unilateral neutral backbone; ANP, asymmetric neutral patch.

‡To whom reprint requests should be addressed. E-mail: robinson@chem.washington.edu.

The publication costs of this article were defrayed in part by page charge payment. This article must therefore be hereby marked "*advertisement*" in accordance with 18 U.S.C. §1734 solely to indicate this fact.

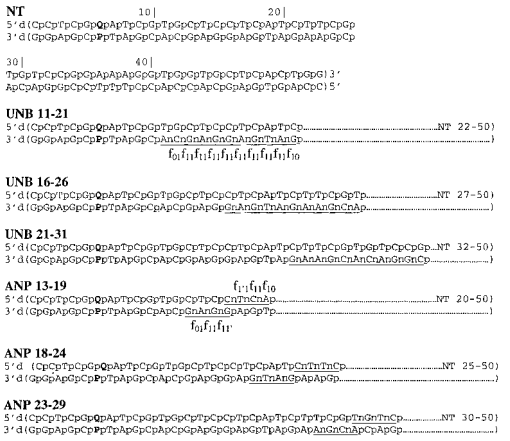

Fig. 1. List of all 50-mer sequences tested for probe dynamics and differing only by MP placement. Neutralized regions (n indicates MP) are underlined. NT is the control and contains no MPs. Each duplex in the UNB series contains ten 3′-MPs in a row on the **P**-containing strand. Each duplex in the ANP series contains six 3′-MP-modified bases, asymmetrically placed along both strands (Fig. 2). The associated flexibility parameters are shown: $f_{01} = f_{10}$ indicates an MP with one MP neighbor, f_{11} indicates an MP with an MP neighbor on each side, and $f_{11'}$ indicates an MP with an MP neighbor on one side on the same strand and an MP neighbor on the other side on the opposite strand (see also text).

To investigate differential DNA flexibility, we define $\bar{\kappa}$ as a mean force constant, then f_i as the flexibility parameter for the ith base pair: $f_i = (\bar{\kappa} - \kappa_i)/\bar{\kappa}$ (Fig. 1). A positive flexibility corresponds to a sequence locally more flexible than average. To determine the impact of MP substitution on duplex DNA flexibility, we measured the relative flexibilities of a series of DNAs, all of which have the same sequence (17), length, and spin-label at the sixth base pair (Fig. 1). The DNAs differ only by MP substitution in test regions that are never closer to the spin-labeled base pair than 5 bp.

Materials and Methods

The spin probe used in this work, **Q**, was prepared as previously described (18, 19), using both the naturally abundant [^{14}N,^{1}H$_{12}$] and the isotopically substituted [^{15}N,^{2}H$_{12}$] nitroxides. **Q** was site-specifically attached at the sixth position of every 50-mer duplex DNA sampled. All oligomers were synthesized on an ABS 392 DNA synthesizer (Applied Biosystems) and purified by using reverse-phase (trityl-on purification) high-pressure liquid chromatography on a Dynamax 300-Å column or denaturing polyacrylamide gel electrophoresis. Oligonucleotides containing site-specific racemic MP substitutions were synthesized with methylphosphonamidite monomers (Glen Research) at the 2 μmol scale, using acetyl-protected deoxycytosine (dC) (Glen Research), and manually deprotected and removed from the solid support by using a modified deprotection procedure (Glen Research).

The UNB (neutral backbone, 1-side only) series was synthesized as complementary 50-mer strands and appropriately annealed to their corresponding partners to form the duplexes. The ANP (neutral backbone, asymmetric patch) series was produced by annealing 4 nmol each of the 11-mer primer strand containing **Q** and of the chemically phosphorylated (CPRII) (Glen Research) 39-mer containing three MPs to the appropriate template 50-mer containing the other three MPs. The 11-mer and 39-mer were ligated with T4 DNA ligase in 200 μl of T4 DNA ligase buffer (GIBCO/BRL) on a 16°C block followed by polyacrylamide gel electrophoresis purification at room temperature. The DNA was extracted from the gel by using the crush-and-soak procedure (24) in duplex elution buffer (0.5 M ammonium acetate/10 mM $MgCl_2$/10 mM Na_2 EDTA). Extracted DNA was precipitated with ethanol (24), dried, and redissolved in 10 μl of PNE buffer (0.01 M sodium phosphate, pH 7.0/0.1 M NaCl/0.1 mM EDTA).

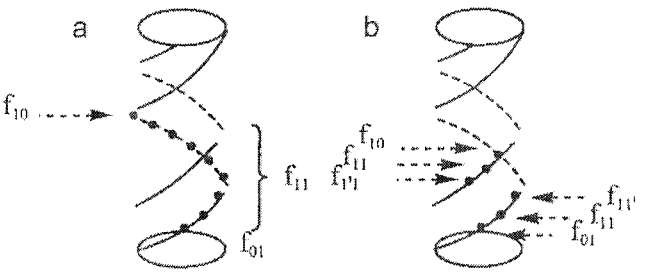

Fig. 2. MP placement (●) along the DNA backbone in the UNB series (*a*) and in the ANP series (*b*). (See Fig. 1 legend for $f_{01} = f_{10}$, f_{11}, and $f_{1'1} = f_{11'}$.)

The continuous-wave electron paramagnetic resonance (CW-EPR) spectra were digitally recorded on a commercial Bruker EMX spectrometer with Varian TE102 cavity (Bruker, Billerica, MA). Parameters used for CW-EPR measurements include 10 and 100 kHz modulation frequency, 1.0 G modulation amplitude, 1–5 mW power (nonsaturating conditions), 1,024 points, and 30°C regulated to ±0.2°C (well below melting temperature, T_m, for these molecules). Line samples of 200–300 μM duplex DNA were prepared in either a 0.6 × 0.84 mm or 0.8 × 1.0 mm quartz capillary and stored at 4°C between EPR measurements. Rigid limit **A** and **g** tensors obtained elsewhere (16) and calculated rotational correlation times (23) were used to simulate the spectra of the B-form 50-mers in PNE solution at 30°C. $\langle\beta_i^2\rangle$ was found by best fitting the outer components of the spectra and then fit with the weakly bending rod theory (16, 17, 21, 22) to determine the force constant κ_i at the MP-modified locations. The correlation coefficient for the simulations to the experimental spectra (20) exceeded 0.97 for all spectra.

Thermodynamic data were collected on a Beckman DU 650 spectrophotometer monitoring the absorbance at 260 nm from 20°C to 95°C (data not shown). Experiments were analyzed in MATLAB for T_m and ΔH according to the Breslauer method described in ref. 25. Circular dichroism (CD) was measured on a Jasco J720 spectropolarimeter monitored from 340 nm to 200 nm at 30.0 ± 0.2°C (data not shown). PNE buffer was used in all experiments.

Results

Two types of MP substitutions are studied (Figs. 1 and 2): (*i*) MPs are placed in a 10-bp stretch on the strand containing the base-**P**, creating a unilateral neutral backbone (UNB) region; and (*ii*) six MPs in total are placed on both strands, three per strand, situated across the minor groove as an asymmetric neutral patch (ANP) (2). The flexibility of the UNB and ANP series of DNAs is reported in terms of the flexibility of the probe at base pair 6, $\langle\beta_6^2\rangle$. Fig. 3 shows the high-field region of the EPR spectra of three different MP substitutions (Fig. 1). The low-field turning points (not shown) are aligned to the same magnetic field. The spectra show that the position of the high-field line is sensitive to the MP substitution: the line's position increases with increasing distance of MP substitution from the probe (**Q**). Fig. 4 plots the values of $\langle\beta_6^2\rangle$ as a function of the position of the base pair containing the MP closest to the probe.

For both the ANP and UNB series, the $\langle\beta_6^2\rangle$ values for the two DNAs containing MPs closest to the **Q·P** base pair are the largest, and they monotonically decrease as the MP-containing region is placed farther from the **Q·P** base pair. All MP-containing sequences have $\langle\beta_6^2\rangle$ values greater than or equal to

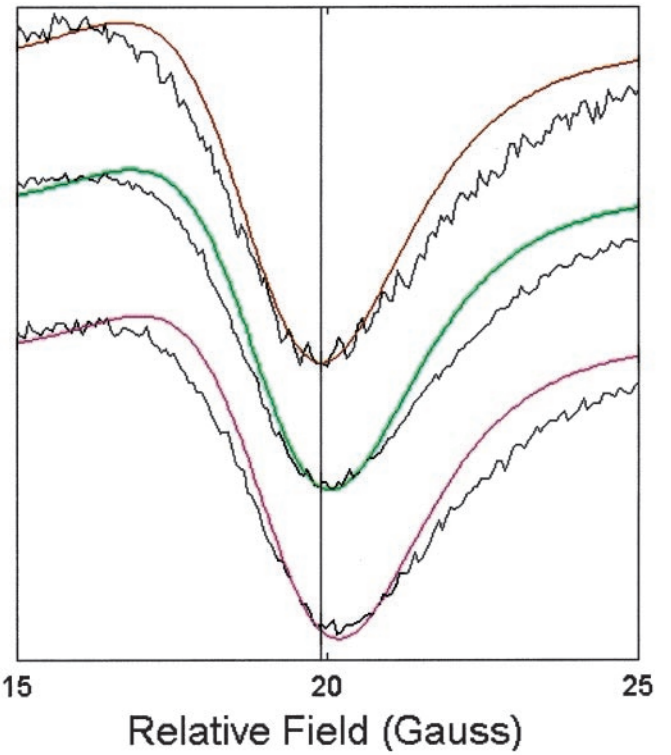

Fig. 3. EPR spectra of the three duplex DNAs in the UNB series (Fig. 1): from top to bottom, UNB 11–21, UNB 16–26, and UNB 21–31. The positions of the center of the high-field lines of the three spectra differ by ≈150 mG (1 mG = 0.1 μT). The vertical line aids the eye to see the differences. Overlaid on each spectrum is the theoretical simulation. Multiple experiments show reproducibility to better than 40 mG.

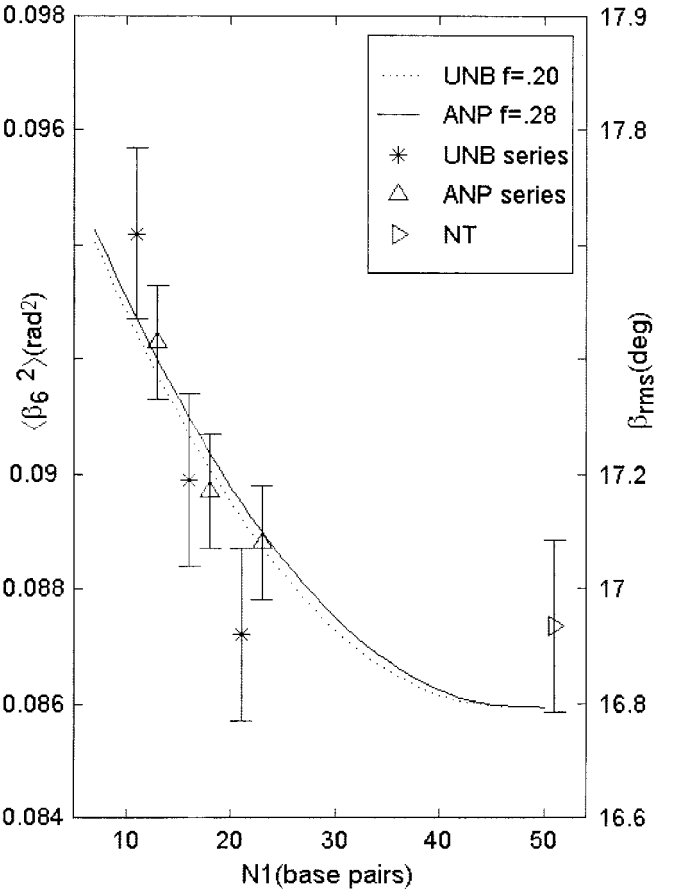

Fig. 4. The mean squared librational amplitude, $\langle\beta_6^2(\infty)\rangle$, in radians^2 (displayed on the left) and the amplitude in degrees (displayed on the right) are plotted against the MP start position (in base pairs). The UNB series (✳) and the ANP series (△) are overlaid with calculated curves (17) by using the individual best-fit flexibility parameters, $f_{UNB} = 0.20 \pm 0.04$ (solid line) and $f_{ANP} = 0.28 \pm 0.05$ (dotted line). Errors on $\langle\beta_6^2(\infty)\rangle$ do not exceed ± 0.0015 rad^2. The best-fit NT $\langle\beta_6^2(\infty)\rangle$ value (◁) is 0.0860 rad^2, where $\langle\beta_6^2(\infty)\rangle = 0.0219$ rad^2. $\langle\Delta\beta^2\rangle = kT/\bar{\kappa} = 0.00272$ rad^2, as determined before (17).

the control DNA, within experimental error, indicating that this type of modification of the backbone increases DNA flexibility over the native polyanionic form. Both increased and decreased values in $\langle\beta_6^2\rangle$ have been observed in other DNAs, depending on the substitution (17, 26).

The $\langle\beta_6^2\rangle$ values (Fig. 4) were then used to estimate a flexibility parameter, f_i, for the ith base pair for both the UNB and the ANP series as follows: the value of $\bar{\kappa}$ was determined previously (17), and f_i for a native phosphate linkage is taken to be zero. Initially we assume that the flexibility parameter for an MP linkage is a single nonzero value and is equal to every other MP linkage in the sample type, UNB or ANP, determined by a least-squares criterion (see Fig. 1). The data from the UNB and the ANP series (Fig. 4) were analyzed independently, each yielding a distinct flexibility parameter (Fig. 4 legend). The difference between the flexibilities of these two series, even when considering the errors, suggests that they are distinguishable.

To understand better the flexibility difference between these two series, the data were reanalyzed to account for the different environments of MP substitutions. A subscript m or n, is used for f_{mn}, where m and n are, respectively, the number of MPs on the base pair to the 5′ and 3′ side of the MP under consideration. m' or n' indicates that the neighboring MP is on the opposite strand (Fig. 2). The flexibility parameter of the base pairs beginning and ending the neutral region in the UNB series, $f_{10} = f_{01}$, is, for simplicity, assumed to be half that of the ones in the interior of the MP sequence in the UNB series. The best-fit flexibility parameter, $f_{11} = 0.19 \pm 0.03$, is nearly unchanged from the previous analysis of the MP series, which used a single flexibility parameter. Moreover, we assume the flexibilities from the UNB series apply to the ANP series for the MPs that have the same types of MP neighbors. The flexibility of the central pair of the ANP series, $f_{11'}$, is the only one that is different, and it does not differ in charge density but only in charge placement. Fitting the data in Fig. 4 to this model yields a flexibility parameter $f_{11'} = 0.41 \pm 0.03$. This result suggests that an MP-containing base pair with two flanking MPs, one on each strand, is more flexible than one with two flanking MPs on the same strand. Repeating the analysis with the assumption that $f_{10} = f_{11}$ did not significantly change the value of the $f_{11'}$.

The finding that $f_{11'} \cong 2f_{11}$ implies that the spatial organization of the MPs is an important component of the flexibility. The MPs in the UNB series are locally nearly aligned (each being rotated by 34.6° from its neighbor) with the helix axis, whereas the MPs that cross from one strand to the other in the ANP series are rotated by more than 90° (Fig. 2). This effect of spatial arrangement of MPs suggests that the bending is anisotropic, and that the increased flexibility of the UNB series is in the direction of the substitution. The central bases of the ANP have MP substitution in one direction on one side and perpendicular substitution on the other side. One might, then, expect that replacing both phosphates with MPs would approximately double the flexibility and also increase flexibility in two dimensions.

Discussion

There are two important physical parameters associated with changes in local flexibility: the breadth of the local radius of

curvature and the change in entropy. First, the radius of curvature for DNA found in the nucleosome is ≈45 Å, which corresponds to a 4.3° bend per base pair. Net curvature requires that the bends persist in the same direction (or within 90° of one another). For a straight-chain DNA undergoing average dynamic bending, characterized by $\langle \Delta\beta^2 \rangle$ (17), the Boltzmann distribution predicts that only ≈7% of the base pairs would exist at any given time in the correct configuration to accommodate the histone. Strauss and Maher (3, 4) measured static bends caused by MP substitution on the order of 3°, which correspond to a radius of curvature of 60 Å. Preexisting unidirectional 3° bends undergoing the same dynamic bending increase the frequency of finding 4.3° bends in one direction to 33% of the base pairs. The results herein add a 1.2- and 1.4-fold increase in flexibility of the DNA at the MP sites, depending on whether the substitution is unilateral or asymmetric, respectively. This additional flexibility to the assumed 3° static bends (2–4) further increases the frequency of the 4.3° bends to 35% and 37% in one direction for the two types of substitutions. These results suggest that the combination of static and dynamic bends associated with charge neutralization (15) makes an important contribution to the nucleosomal packaging of DNA. In light of these results, it is likely that a number of processes—including the binding of multivalent cations, transcription factors, and architectural proteins to DNA—are facilitated by a combination of dynamic and static structural changes arising from charge neutralization (27–29). As an example, high mobility group (HMG) proteins have been found to bind to architectural type DNA motifs, such as *cis*-diamminedichloroplatinum(II) (cisplatin)-modified DNA, with dramatically higher affinities than to sequence-specific sites (30). Our own investigations have revealed that one cisplatin lesion increases the local flexibility of the DNA almost 2-fold (26), leaving one to consider that perhaps an increase in flexibility can be an important, if not the determining, mechanism in such high-affinity binding.

Second, a change in entropy occurs upon MP substitution. From the Hookeian potential governing bending in both x and y directions, where z is aligned along the DNA helix (16), and from the assumption that force constants are temperature independent (16), it follows that MP-induced changes in the bending force constants cause the entropy to change, but not the enthalpy. The change in entropy, ΔS, attributable to the MP substitution, as a function of the flexibility parameters is

$$\Delta S = -R \sum_{i=1}^{N} \ln(1 - f_i) \cong R \sum_{i=1}^{N} f_i ,$$

where $f_i \leq 0.3$ and R is the gas constant. This term predicts that the free energy of the UNB series is entropically lowered by about 5.7 kJ/mol at 30°C. From a thermodynamic perspective then, the increase in entropy could participate in stabilizing the neutralized intermediate along the pathway to protein binding, or contribute to the stability of entropically favored protein binding, such as is the case of the binding of TATA box-binding protein (TBP) to DNA (31).

We now consider whether the effects of MP substitution can be explained in terms of electrostatic forces. Certainly a large body of experimental literature suggests that the observed structural effects directly correlate to the magnitude of the charge modification at the DNA backbone (even at 0.1 M salt) (2–6, 32). With the majority of theoretical studies discounting electrostatics at the backbone as a significant contributor to static bending (or increased flexing), it becomes difficult to decide the issue (9–15). Therefore, we examined the UV melting profiles (Table 1) and the CD structure of representative MP substituted sequences (see Fig. 1).

Table 1. Thermodynamic data

Name	T_m, °C	ΔH, kcal/mol	ΔS, cal/mol·K	ΔG at 30°C, kcal/mol
ANP 13–19	81.1 ± 1.1	122 ± 20	344 ± 57	18 ± 20
UNB 16–26	81.8 ± 0.4	133 ± 17	375 ± 48	19 ± 17
NT	86.9 ± 1.6	241 ± 18	669 ± 52	38 ± 18

Data were derived from UV melting curves (absorbance at 260 nm) for native and MP-substituted DNA going from duplex to single-strand forms for ANP 13–19, UNB 16–26, and the control NT (see Fig. 1) from 20°C to 95°C in PNE buffer (10 mM sodium phosphate/100 mM NaCl/0.1 mM EDTA, pH 7.0).

The electrostatic effect on melting duplex DNA predicts that T_m for a partially uncharged duplex would increase compared with the fully charged DNA because there is less charge repulsion to destabilize the duplex (33). ΔG for MP-substituted DNA should also increase upon melting compared with the charged duplex because of MP stabilization. ΔH for MP-substituted DNA would then decrease compared with that for the charged duplex because of the temperature dependence of the dielectric constant, a characteristic of water. ΔH for the uncharged molecule should be less than for the neutral strand, but ΔG should be greater by the relations

$$\Delta H^{\text{elect}} = \frac{\partial(\Delta G^{\text{elect}}/T)}{\partial(1/T)} \qquad [2]$$

and

$$\frac{\Delta G^{\text{elect}}}{T} = \frac{\alpha}{\varepsilon T} \simeq \alpha' \left(\frac{1}{T}\right)^{-1/3}, \qquad [3]$$

where ε is the dielectric constant of water and α and α' contain all temperature-independent screened-coulomb effects. Therefore,

$$\Delta H^{\text{elect}} = -\frac{1}{3} \cdot \alpha' \left(\frac{1}{T}\right)^{-1/3} \cdot \left(\frac{1}{T}\right)^{-1} = -\frac{1}{3} \cdot \Delta G^{\text{elect}} < 0. \qquad [4]$$

One can see that if $\Delta\Delta H$ is negative, $\Delta\Delta G$ must be positive when going from a charged to an uncharged state. For both MP-substituted series, ΔH and ΔG decreased by almost 50% and T_m decreased by ≈5°C relative to the charged DNA (see Table 1). The reduction in ΔH is consistent with an electrostatic effect, but the reduction in T_m and ΔG is not. These results are consistent with those of Reynolds *et al.* (34), who studied natural phosphate and MP-substituted DNA·RNA hybrids in 0.1 M salt and found the same trends in T_m, ΔH, and ΔG as reported here. Quartin and Wetmur (32) observed decreases in T_m in high (20 mM to 1 M) salt but increases in T_m at low salt (less than 4 mM) for short MP-containing duplexes, implying that the electrostatics dominate the energetics of DNA melting at low salt but play a minor role at high salt. At low salt, the electrostatics overcome structural perturbations introduced by MP substitution predicted by molecular mechanics and observed by CD (discussed below). Moody and co-workers (35) melted d(MP-C)$_5$ on poly(dG), producing a DNA configuration significantly different from ours, and found increases in both ΔH and T_m, inconsistent with the idea that melting is dominated by electrostatics. At the physiological conditions that Strauss and Maher, Quartin and Wetmur, Reynolds *et al.,* and our laboratory used (≈0.1 M salt), the melting and CD data indicate that MP effects are not purely electrostatic.

It appears that at higher salt concentrations (≈0.1 M) the charge neutralization by itself is not sufficient to induce the magnitude of bends measured upon MP substitution. Nevertheless, such bends are induced. Molecular mechanics calcu-

lations predict that MP substitution renders that region of the duplex hydrophobic and changes the widths of the minor and major grooves (33). CD spectra of NT, ANP 13–19, and UNB 16–26 (Fig. 1 and data not shown) taken under the same conditions as the EPR experiments were very similar but showed differences of about 10–20% from 240 to 280 nm, indicating alteration of the secondary structure equal to the amount of MP substitution (which is 10–20% of the DNA). The combined findings suggest that MP substitution introduces structural as well as dynamic changes in duplex DNA that mimic protein interactions beyond what is predicted by electrostatics. The presence of the methyl group in pure R_P-isomer or in a racemic R_P and S_P mixture of MP-substituted duplex DNA is predicted to narrow the minor groove (33). Basic residues in the CAP protein (36) and the nucleosome (37) make phosphate contacts to narrowed minor groove DNA that is bent toward the protein surface, much as the neutral patch DNA mimics minor groove bending in DNA. Hydrophobic regions caused by MP substitutions may also mimic regions of excluded waters in protein–DNA complexes, undoubtedly contributing to the energetics of binding. We suggest that hydrophobic and structural perturbations of this sort are important components of the charge-neutralizing process of regulatory proteins when bending and binding to DNA. Thus MP substitution is a good example of duplex DNA's polymorphic behavior, and is an appropriate model for protein modification.

In summary, asymmetric phosphate neutralization has been suggested to be a highly conserved and common mechanism in protein–DNA recognition. Not only are structural bends induced by MP substitutions (2, 3), but also our experiments show that the dynamics of such bends are greater than in native DNA. We have previously shown (17) that the range in flexibilities for native charged duplex DNA attributable to sequence is about 30%. MP substitution along one strand in the duplex increases the flexibility by more than 20%, and substitution along both strands in the duplex increases the flexibility by more than 40% (which may not be exclusive of sequence). Phosphate neutralization dynamics plays an important role in the energetics of protein binding in that flexibility increases the rms extent of bending without additional energy, and suggests that a partially uncharged duplex DNA may be an intermediate along the protein-binding pathway. The additional flexibility entropically stabilizes this structure, and hence, this mechanism may play an important role in protein–DNA recognition by increasing local flexibility to accommodate dynamic bending and steric relief as well as introducing flexible bends for architectural type protein binding.

We are grateful to Drs. J. M. Schurr and S. Th. Sigurdsson for reading this manuscript and many helpful suggestions. This work was supported in part by National Institute of General Medical Sciences Grants GM 32681 and GM 55963 and National Institute on Environmental Health Sciences Environmental Sciences Center Grant P30 ESO7033.

1. Mirzabekov, A. D. & Rich, A. (1979) *Proc. Natl. Acad. Sci. USA* **76,** 1118–1121.
2. Strauss, J. K. & Maher, L. J., III (1994) *Science* **266,** 1829–1834.
3. Strauss-Soukup, J. K., Vaghefi, M. M., Hogrefe, R. I. & Maher, L. J., III (1997) *Biochemistry* **36,** 8692–8698.
4. Strauss-Soukup, J. K., Rodrigues, P. D. & Maher, L. J., III (1998) *Biophys. Chem.* **72,** 297–306.
5. Strauss-Soukup, J. K. & Maher, L. J., III (1998) *Biochemistry* **37,** 1060–1066.
6. Strauss-Soukup, J. K. & Maher, L. J., III (1997) *Biochemistry* **36,** 10026–10032.
7. Strauss-Soukup, J. K. & Maher, L. J., III (1997) *J. Biol. Chem.* **272,** 31570–31575.
8. Hagerman, K. R. & Hagerman, P. J. (1996) *J. Mol. Biol.* **260,** 207–223.
9. Freidman, R. A. & Honig, B. (1992) *Biopolymers* **32,** 145–159.
10. Sivolob, A. & Khrapunov, S. N. (1997) *Biophys. Chem.* **67,** 85–96.
11. Lamm, G., Wong, L. & Pack, G. R. (1994) *Biopolymers* **34,** 227–237.
12. Manning, G. S., Ebralidse, K. K., Mirzabekov, A. D. & Rich, A. (1989) *J. Biomol. Struct. Dyn.* **6,** 877–889.
13. Schurr, J. M. & Schmitz, K. S. (1986) *Annu. Rev. Phys. Chem.* **37,** 271–306.
14. Odijk, T. & Houwaart, A. C. (1978) *J. Polym. Sci. Polym. Phys. Ed.* **16,** 627–639.
15. Gurlie, R. & Zakrzewska, K. (1998) *J. Biomol. Struct. Dyn.* **16,** 605–618.
16. Okonogi, T. M., Reese, A. W., Alley, S. C., Hopkins, P. B. & Robinson, B. H. (1999) *Biophys. J.* **77,** 3256–3276.
17. Okonogi, T. M., Alley, S. C., Reese, A. W., Hopkins, P. B. & Robinson, B. H. (2000) *Biophys. J.* **78,** 2560–2571.
18. Miller, T. R., Alley, S. C., Reese, A. W., Solomon, M. S., McCallister, W. V., Mailer, C., Robinson, B. H. & Hopkins, P. B. (1995) *J. Am. Chem. Soc.* **117,** 9377–9378.
19. Miller, T. R. & Hopkins, B. H. (1994) *Bioorg. Med. Chem. Lett.* **4,** 981–986.
20. Hustedt, E. J., Spaltenstein, A., Kirchner, J. J., Hopkins, P. B. & Robinson, B. H. (1993) *Biochemistry* **32,** 1774–1787.
21. Wu, P., Fujimoto, B. S. & Schurr, J. M. (1987) *Biopolymers* **26,** 1463–1488.
22. Song, L. & Schurr, J. M. (1990) *Biopolymers* **30,** 229–237.
23. Tirado, M. M. & Garcia de la Torre, J. (1980) *J. Chem. Phys.* **73,** 1986–1993.
24. Maniatis, T., Fritsch, E. F. & Sambrook, J. (1989) *Molecular Cloning: A Laboratory Manual* (Cold Spring Harbor Lab. Press, Plainview, NY).
25. Breslauer, K. J. (1994) in *Methods in Molecular Biology*, ed. Agrawal, S. (Humana, Totowa, NJ), Vol. **26,** pp. 347–372.
26. Okonogi, T. M. (2000) Ph.D. dissertation (Univ. of Washington, Seattle).
27. Huang, H., Zhu, L., Reid, B. R., Drobny, G. P. & Hopkins, P. B. (1995) *Science* **270,** 1842–1845.
28. Widom, J. (1998) *Annu. Rev. Biophys. Biomol. Struct.* **27,** 285–327.
29. Bloomfield, V. A. (1997) *Biopolymers* **44,** 269–282.
30. Dunham, S. U. & Lippard, S. J. (1997) *Biochemistry* **36,** 11428–11436.
31. Patikoglou, G. & Burley, S. K. (1997) *Annu. Rev. Biophys. Biomol. Struct.* **26,** 289–325.
32. Quartin, R. S. & Wetmur, J. G. (1988) *Biochemistry* **28,** 1040–1047.
33. Swarnalatha, Y. & Yathindra, N. (1993) *J. Biomol. Struct. Dyn.* **10,** 1023–1045.
34. Reynolds, M. A., Hogrefe, R. I., Jaeger, J. A., Schwartz, D. A., Riley, T. A., Marvin, W. B., Daily, W. J., Vaghefi, M. M., Beck, T. A., Knowles, S. K., *et al.* (1996) *Nucleic Acids Res.* **24,** 4584–4591.
35. Moody, M. R., van Genderen, M. H. P. & Buck, H. M. (1990) *Biopolymers* **30,** 609–618.
36. Schultz, S. C., Shields, G. C. & Steitz, T. A. (1991) *Science* **253,** 1001–1007.
37. Luger, K., Mader, A. W., Richmond, R. K., Sargent, D. F. & Richmond, T. J. (1997) *Nature (London)* **389,** 251–260.